

# In-Situ Optical Absorbance Spectroscopy of Molecular Layers in Carbon Based Molecular Electronic Devices

Andrew P. Bonifas<sup>†,‡</sup> and Richard L. McCreery<sup>\*,‡,§</sup>

Department of Materials Science and Engineering, The Ohio State University, 2041 College Road, Columbus, Ohio 43210, National Institute for Nanotechnology, National Research Council of Canada, Canada T6G 2G2, and Department of Chemistry, University of Alberta, Edmonton, Alberta, Canada T6G 2R3

Received December 18, 2007. Revised Manuscript Received March 17, 2008

In-situ optical absorbance spectroscopy was used to monitor transparent carbon based molecular electronic junctions with various molecular and metal oxide layers. Junctions with molecular layers consisting of *N*-decylamine (C<sub>10</sub>N) and fluorene (FL) did not show absorbance changes upon the application of voltage pulses. Junctions with molecular layers consisting of 4-nitroazobenzene (NAB) and 9,10-anthraquinone (AQ) showed absorbance changes upon the application of voltage pulses which were reversible for at least tens of cycles. For NAB junctions, a negative voltage pulse caused an increase in absorbance at 410 nm and a decrease in absorbance at 360 nm. For AQ junctions, a negative voltage pulse caused an absorbance increase at 395 nm and a decrease in absorbance at 320–350 nm. These absorbance changes are consistent with the reduction of the NAB and AQ layers when the carbon substrate is biased negative. Positive voltage pulses reversed the absorbance changes observed during a negative pulse which is consistent with the reoxidation of the molecular layer. The persistence of the absorbance changes depended strongly on the molecule, with absorbance changes persisting for tens of minutes for NAB junctions but only several seconds for AQ junctions. The in-situ optical absorption results are supported with solution based electrochemistry of both free molecules and chemisorbed molecular layers and time-dependent density functional theory. We have shown that in-situ optical absorbance spectroscopy can be used to probe changes in energy levels through absorption changes in biased molecular junctions, which should be useful for deducing structural and electronic changes that strongly effect electron transfer in molecular electronic devices.

## Introduction

As the field of molecular electronics matures, focus should change from the discovery of novel molecular based architectures to understanding the mechanisms behind the electronic properties of these architectures. Molecular based devices have been reported to exhibit many electronically important characteristics such as negative differential resistance,<sup>1–3</sup> conductance switching,<sup>4,5</sup> rectification,<sup>6–8</sup> and

bistability.<sup>9,10</sup> A fundamental question behind these observed characteristics is if they are influenced by the quantized energy levels of the molecules, a significant driving force behind the excitement in this field. Optical spectroscopy is an attractive method to probe energy levels and molecular structures within molecular devices containing 10<sup>3</sup>–10<sup>12</sup> molecules. Optical absorption (UV–vis), FTIR, and Raman spectroscopy allow direct, nondestructive measurements of molecular properties such as energy levels, oxidation states, and molecular structure which are difficult to obtain from current–voltage or capacitance–voltage measurements alone. In addition, optical spectroscopy often provides fast time resolution for in-situ monitoring of functioning devices. The well established field of spectroelectrochemistry has exploited optical spectroscopy for monitoring molecules in electrochemical cells and thin films allowing complementary structural and electrochemical analysis.<sup>11,12</sup> The current investigation describes the application of some of the principles of spectroelectrochemistry to solid state molecular

\* Corresponding author Tel.: 780-641-1760. E-mail: richard.mcCreery@ualberta.ca.

<sup>†</sup> The Ohio State University.

<sup>‡</sup> National Research Council of Canada.

<sup>§</sup> University of Alberta.

- (1) Chen, J.; Reed, M. A.; Rawlett, A. M.; Tour, J. M. *Science* **1999**, *286*, 1550–1552.
- (2) Chen, F.; He, J.; Nuckolls, C.; Roberts, T.; Klare, J. E.; Lindsay, S. *Nano Lett.* **2005**, *5*, 503–506.
- (3) Kiehl, R. A.; Le, J. D.; Candra, P.; Hoye, R. C.; Hoye, T. R. *Appl. Phys. Lett.* **2006**, *88*.
- (4) Chen, J.; Wang, W.; Klemic, J.; Reed, M. A.; Axelrod, B. W.; Kaschak, D. M.; Rawlett, A. M.; Price, D. W.; Dirk, S. M.; Tour, J. M.; Grubisha, D. S.; Bennett, D. W. *Molecular Electronics II*; New York Academy of Sciences: New York, 2002; Vol. 960, pp 69–99.
- (5) Blum, A. S.; Kushmerick, J. G.; Long, D. P.; Patterson, C. H.; Yang, J. C.; Henderson, J. C.; Yao, Y. X.; Tour, J. M.; Shashidhar, R.; Ratna, B. R. *Nat. Mater.* **2005**, *4*, 167–172.
- (6) Martin, A. S.; Sambles, J. R.; Ashwell, G. J. *Phys. Rev. Lett.* **1993**, *70*, 218–221.
- (7) Chabinye, M. L.; Chen, X. X.; Holmlin, R. E.; Jacobs, H.; Skulason, H.; Frisbie, C. D.; Mujica, V.; Ratner, M. A.; Rampi, M. A.; Whitesides, G. M. *J. Am. Chem. Soc.* **2002**, *124*, 11730–11736.

- (8) Kalakodimi, R. P.; Nowak, A. M.; McCreery, R. L. *Chem. Mater.* **2005**, *17*, 4939–4948.
- (9) Jang, S. S.; Jang, Y. H.; Kim, Y. H.; Goddard, W. A.; Flood, A. H.; Laursen, B. W.; Tseng, H. R.; Stoddart, J. F.; Jeppesen, J. O.; Choi, J. W.; Steuerman, D. W.; DeLonno, E.; Heath, J. R. *J. Am. Chem. Soc.* **2005**, *127*, 1563–1575.
- (10) Lortscher, E.; Cizek, J. W.; Tour, J.; Riel, H. *Small* **2006**, *2*, 973–977.

electronic devices to probe the electronic properties of molecular layers only a few nanometers thick.

We have previously reported the use of in-situ Raman spectroscopy to monitor the molecular structures of chemisorbed molecular layers both in solution and solid state devices.<sup>13,14</sup> Nitroazobenzene molecules chemisorbed on a carbon electrode in an electrolytic solution exhibited reversible changes in their Raman spectrum when the electrode was cycled between reducing and oxidizing potentials. Analysis of the Raman spectra and voltammetry allowed the correlation of the vibrational changes with the reduction and oxidation of the chemisorbed molecular layer. In solid state devices, consisting of NAB and TiO<sub>2</sub> between carbon and Au electrodes, Raman spectroscopy revealed vibrational changes consistent with the reduction and oxidation of the molecular layer caused by an applied voltage. Although Raman provides valuable in-situ structural information, it requires the molecular layer to consist of a strong Raman scatterer and be subjected to prolonged laser exposure. FTIR spectroscopy has been used to characterize molecular devices, but in-situ analysis has been limited by signal acquisition times of several minutes.<sup>15–17</sup> In addition, FTIR has limitations on the substrate material where the surface selection rules are most pronounced on Au. Optical absorption has been used to probe conducting polymers in light emitting diodes and metal/polymer/semiconductor structures, but the polymer layers were much thicker (~100 nm) than those used in molecular electronic devices.<sup>18,19</sup>

The motivation for using optical absorption as a diagnostic tool is threefold. First, since many molecular systems of electronic interest absorb in the ultraviolet–visible region, optical absorption allows for the analysis of a wide range of molecular systems. Metal oxides in molecule/metal oxide “heterojunctions” are also amenable to optical absorption spectroscopy. Second, time resolution of optical absorption may range from femtoseconds to seconds for laser based techniques or microseconds to seconds with broadband light sources. Considering the speed of most electronic devices, fast time resolution is necessary for in-situ analysis of junction dynamics. Third, optical absorption gives direct evidence of energy level changes within an electronically active device. Although the absorption wavelength does not necessarily directly relate to the HOMO–LUMO gap in the molecular layer, it does give insight to how energy levels change with time. By measuring absorption as a function of applied voltage or time, significant insight into electron

transfer and energy level alignment between device layers can be obtained. For these reasons, optical absorption spectroscopy should be a useful in-situ probe of molecular electronic devices provided the device structure is amenable to spectroscopy of the “buried interface”.

An initial question is what scale of absorbance changes should be expected from a device with a redox active molecular layer in the nanometer thickness range. An estimated absorbance change associated with a redox reaction is given by a modified Beer–Lambert equation:

$$\Delta A(\lambda) = \sum_{i=1}^{i=n} \epsilon(\lambda)_i b \Delta C_i = \sum_{i=1}^{i=n} \epsilon(\lambda)_i \Delta \Gamma_i$$

where  $\epsilon(\lambda)_i$  is the molar absorptivity at wavelength  $\lambda$  of species  $i$ ,  $b$  is the path length,  $\Delta C_i$  is the change in concentration,  $\Delta \Gamma_i$  is the change in surface concentration, and  $n$  is the number of absorbing species. Assuming  $\Gamma = 1 \times 10^{-10} \text{ mol} \cdot \text{cm}^{-2}$  and  $\epsilon_{\text{anion}} = 1 \times 10^4 \text{ M}^{-1} \cdot \text{cm}^{-1}$  ( $1 \times 10^7 \text{ cm}^2 \cdot \text{mol}^{-1}$ ), the absorbance change would be  $1 \times 10^{-3}$  for complete reduction of a monolayer to its anion, which is higher than the limit of detection for sensitive optical absorption spectrometers. Although optical absorption is not necessarily linear with the number of chromophores in dense molecular layers, as is the case for dilute solutions, the above calculation gives a rough estimate of the expected absorbance change.

The molecular junctions that were investigated in this study had a similar architecture to our previous carbon/molecule/metal oxide/Au junctions.<sup>20,21</sup> To allow optical transmission, the opaque carbon based pyrolyzed photoresist films (PPF) used previously were replaced with optically transparent electron beam evaporated carbon films, which have been shown to have electrochemical properties similar to those of PPF.<sup>22</sup> The oxide layer, SiO<sub>2</sub> or Al<sub>2</sub>O<sub>3</sub>, behaved as an electron barrier prohibiting DC conduction through the junctions allowing the junctions to operate in the coulomb blockade (CB) regime. As has been shown experimentally and proposed theoretically, junctions operating in the CB regime can exhibit redox reactions analogous to conventional electrochemistry.<sup>14,21,23,24</sup>

In the current investigation, we used in-situ optical absorbance spectroscopy to investigate the molecular layer in molecule/oxide junctions. Application of voltage pulses resulted in reversible absorbance changes which are consistent with changes in the oxidation state of the molecular layer. Identification of the oxidation state and energy levels within the molecular layer is critical to understanding electron transfer properties within molecular devices. To our knowledge, these in-situ optical absorption spectra are the first reported for a nanometer thick molecular layer in an active solid state molecular junction. These results provide evidence

- (11) Gale, R. J. *Spectroelectrochemistry, Theory and Practice*; Plenum Press: New York, 1988.
- (12) Ruiz, V.; Colina, A.; Heras, M. A.; Lopez-Palacios, J. J. *Phys. Chem. C* **2007**, *111*, 4277–4284.
- (13) Itoh, T.; McCreery, R. L. *J. Am. Chem. Soc.* **2002**, *124*, 10894–10902.
- (14) Nowak, A. M.; McCreery, R. L. *J. Am. Chem. Soc.* **2004**, *126*, 16621–16631.
- (15) de Boer, B.; Meng, H.; Perepichka, D. F.; Zheng, J.; Frank, M. M.; Chabal, Y. J.; Bao, Z. N. *Langmuir* **2003**, *19*, 4272–4284.
- (16) Richter, C. A.; Hacker, C. A.; Richter, L. J. *J. Phys. Chem. B* **2005**, *109*, 21836–21841.
- (17) Richter, C. A.; Hacker, C. A.; Richter, L. J.; Kirillov, O. A.; Suehle, J. S.; Vogel, E. M. *Solid-State Electron.* **2006**, *50*, 1088–1096.
- (18) Brown, T. M.; Kim, J. S.; Friend, R. H.; Cacialli, F.; Daik, R.; Feast, W. J. *Appl. Phys. Lett.* **1999**, *75*, 1679–1681.
- (19) Ziemelis, K. E.; Hussain, A. T.; Bradley, D. D. C.; Friend, R. H.; Ruhe, J.; Wegner, G. *Phys. Rev. Lett.* **1991**, *66*, 2231–2234.

- (20) Ranganathan, S.; Steidel, I.; Anariba, F.; McCreery, R. L. *Nano Lett.* **2001**, *1*, 491–494.
- (21) McCreery, R. L.; Wu, J.; Kalakodimi, R. P. *Phys. Chem. Chem. Phys.* **2006**, *8*, 2572–2590.
- (22) Blackstock, J. J.; Rostami, A. A.; Nowak, A. M.; McCreery, R. L.; Freeman, M. R.; McDermott, M. T. *Anal. Chem.* **2004**, *76*, 2544–2552.
- (23) Lindsay, S. M.; Ratner, M. A. *Adv. Mater.* **2007**, *19*, 23–31.
- (24) Solak, A. O.; Ranganathan, S.; Itoh, T.; McCreery, R. L. *Electrochem. Solid State Lett.* **2002**, *5*, E43–E46.

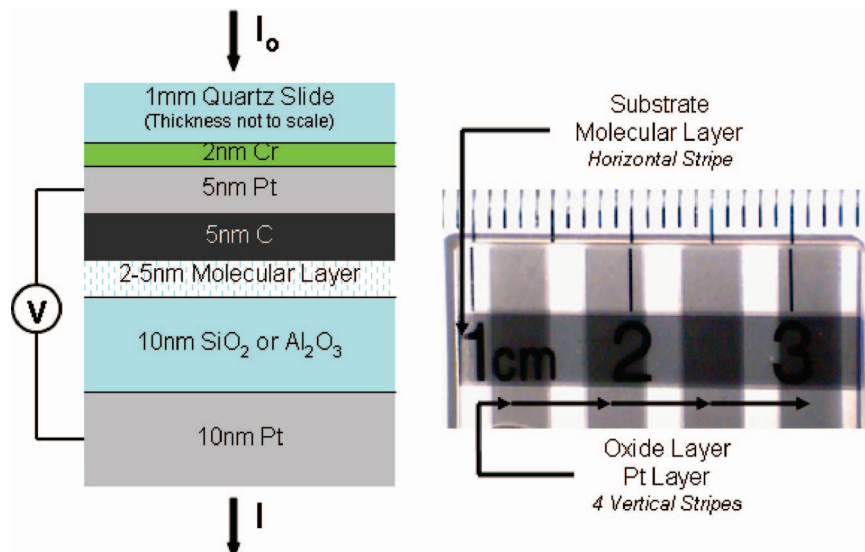


**Figure 1.** Schematic and image of an optically transparent molecular electronic junction.

that the electronic state of a molecular layer can be dynamically changed, which is a significant milestone in confirming the molecular influence on our architecture of molecular junctions.

### Experimental Section

Optically transparent substrates were prepared with electron beam evaporation by successive depositions of 2.0 nm Cr, 5.0 nm Pt, and 5.0 nm C (from graphite rods) on fused quartz slides (G.E. 124, Technical Glass Products). Deposition pressure was  $<5.0 \times 10^{-6}$  torr with a deposition rate of  $0.3 \text{ A} \cdot \text{s}^{-1}$  for all three layers. Atomic force microscopy (AFM) was used in tapping mode to measure the surface roughness of the substrates. A collinear four point probe was used to measure the electrical resistivity of the Pt and C layers. Top oxide/Pt contacts were evaporated through a shadow mask giving a cross bar architecture with an active area of  $0.16 \text{ cm}^2$ . Deposition of 10 nm oxide layers, from either  $\text{SiO}_2$  or  $\text{Al}_2\text{O}_3$ , was performed at an  $\text{O}_2$  backpressure of  $1 \times 10^{-5}$  torr and a rate of  $0.3 \text{ A} \cdot \text{s}^{-1}$ . Pt top contacts, 10 nm thick, were deposited at  $<8.0 \times 10^{-6}$  torr with a rate of  $0.3 \text{ A} \cdot \text{s}^{-1}$  without breaking vacuum after oxide deposition. An image of a final junction is shown in Figure 1. A Perkin-Elmer Lambda 900 UV-vis-NIR spectrometer was used to record the absorbance of the transparent substrates and final junctions relative to a reference quartz slide.

For 4-nitroazobenzene (NAB), 9,10-anthraquinone (AQ), and fluorene (FL) junctions, modification of the transparent substrates was performed through electrochemical reduction of a 1.0 mM solution of the corresponding diazonium salt in acetonitrile (MeCN) containing 0.1 M *n*-tetrabutylammonium tetrafluoroborate ( $\text{TBABF}_4$ ), as described previously.<sup>25,26</sup> *N*-decylamine ( $\text{C}_{10}\text{N}$ ) modification was performed through electrochemical oxidation of 5 mM *N*-decylamine in MeCN containing 0.1 M  $\text{TBABF}_4$  at 1.4 V versus  $\text{Ag}/\text{Ag}^+$  for 10 min.<sup>27,28</sup> Solutions were thoroughly degassed with Ar before modification and blanketed with Ar during modification. Modified substrates were sonicated in MeCN for 5 min to remove physisorbed molecules. Molecular

layer thicknesses were measured using a “scratching” technique with AFM, as described previously.<sup>29</sup>

Solution voltammetry was performed with a BAS/epsilon potentiostat,  $\text{Ag}/\text{Ag}^+$  nonaqueous reference electrode, and a platinum counter electrode. The working electrode was a stationary  $2 \text{ mm}^2$  Au electrode (BAS, MF-2014) modified by evaporating 5.0 nm of both Pt and C successively on the Au electrode to replicate the transparent substrate. To minimize effects caused by oxygen and water, the electrochemistry was performed in a dry nitrogen environment. The MeCN solvent was dried, nitrogen purged, and transferred via a Schlenk line into a nitrogen glovebox. Voltammetry of free NAB and AQ was performed with 1.0 mM solutions in MeCN containing 1.0 M  $\text{TBABF}_4$ . For NAB and AQ layers, voltammetry was performed using NAB and AQ modified electrodes as the working electrodes in 1.0 M  $\text{TBABF}_4$ .

In-situ optical absorbance of the molecular junctions was measured in the absence of a liquid electrolyte. After mounting a junction in a CCD based spectrometer (see below), a reference spectrum without applied bias was collected. Response to an applied bias is stated as delta absorbance ( $\Delta A$ ) which is the change in absorbance relative to the reference spectrum. Since the junction absorbance was 2–3 orders of magnitude larger than the observed  $\Delta A$  ( $\sim 1 \times 10^{-3}$ ), the reference spectrum was set to zero on the  $\Delta A$  scale to permit the observation of small changes in absorption. With this convention, a positive  $\Delta A$  identifies an increase and a negative  $\Delta A$  identifies a decrease in absorbance relative to the reference spectrum.

A custom program in Labview 8.1 (National Instruments) was used to apply voltage pulses to the junctions with the pulse sequence:  $V = 0$  for 30 s;  $V = V_{\text{neg}}$  for 100 ms;  $V = 0$  for 30 s;  $V = V_{\text{pos}}$  for 100 ms; and  $V = 0$  for 30 s, where  $V_{\text{neg}}$  ( $V_{\text{pos}}$ ) is the magnitude of the negative (positive) voltage pulse. In all experiments, the voltage sign convention is the carbon substrate relative to the Pt top contact. After each voltage pulse,  $\Delta A$  was measured while  $V = 0$  during the 30 s wait period. After each pulse sequence, the capacitance of the junction was measured from a current–voltage curve and compared to the initial junction capacitance to ensure dielectric breakdown did not occur during the in-situ measurements. Several examples of current–voltage behavior before and after absorbance monitoring are shown in Supporting Information.

(25) Allongue, P.; Delamar, M.; Desbat, B.; Fagebaume, O.; Hitmi, R.; Pinson, J.; Saveant, J. M. *J. Am. Chem. Soc.* **1997**, *119*, 201–207.

(26) Brooksby, P. A.; Downard, A. J. *J. Phys. Chem. B* **2005**, *109*, 8791–8798.

(27) Hoekstra, K. J.; Bein, T. *Chem. Mater.* **1996**, *8*, 1865–1870.

(28) Downard, A. J. *Electroanalysis* **2000**, *12*, 1085–1096.

(29) Anariba, F.; DuVall, S. H.; McCreery, R. L. *Anal. Chem.* **2003**, *75*, 3837–3844.

In-situ optical absorbance spectra were recorded with a custom built optical absorbance spectrometer. A tungsten-halogen lamp (Sciencetech Inc.) with a very low ripple DC power supply was used as the light source with quartz optics and apertures to transmit a 2.5 mm diameter light pattern through the cross-bar junctions as indicated in Figure 1. Care was taken to restrict the light beam to the active area of the junction. To electrically address the devices in the sample chamber, wires were attached with conducting silver epoxy. Quartz optics were used to match the transmitted light into an f/4 Czerny-Turner spectrograph (Andor, Shamrock SR-303-i-b) with a back-thinned CCD (Andor, Newton DU920N-BU).

Since the expected  $\Delta A$  is in the  $1 \times 10^{-3}$  range, maximizing signal-to-noise ratio was crucial. The CCD was cooled to  $-60^\circ\text{C}$  to minimize thermal noise and full vertical binned (FVB) to maximize the number of counts. Since the CCD camera had a very low readout noise (three counts per FVB readout), binning speed was selected to maximize total counts. Readout and shutter speed limited the maximum number of counts to  $3 \times 10^6$  with a two second integration period at 600 nm. In the shot noise limited regime, the standard deviation of the absorbance is given by modification of an equation presented by Ingle and Crouch<sup>30</sup> in the case where the incident and transmitted intensities are nearly equal:

$$\sigma_A = \sqrt{2}(0.434) \left( \frac{\sqrt{\text{counts}}}{\text{counts}} \right)$$

Assigning the limit of detection (LOD) as three times the standard deviation, LOD is

$$\text{LOD} = 3 \left[ \sqrt{2}(0.434) \left( \frac{\sqrt{\text{counts}}}{\text{counts}} \right) \right]$$

Using the maximum number of counts measured for a 2 s integration period, the LOD is  $1.1 \times 10^{-3}$ . Increasing the integration time to 30 s causes the LOD to decrease to  $2.8 \times 10^{-4}$ . Superpixel integration was used to increase the LOD by effectively increasing the number of counts while keeping the resulting decrease in wavelength resolution ( $<4$  nm) a fraction of the absorption bandwidth. Superpixel integration was critical in wavelength regions where the counts were below the maximum counts, which occurred in the blue region of the spectra. With the use of superpixel integration and relatively small dark signal and readout noise, we are confident to identify the LOD to be  $2.0 \times 10^{-4}$  at all reported wavelengths.

Gaussian '03 was used to perform time dependent density functional theory (TDDFT) [B3LYP/6-31+G(d,p)] to predict total energies, excitation transitions, and orbital energies.<sup>31</sup> Diffuse

**Table 1. Surface Roughness and Sheet Resistance of Deposited Layers on Quartz (Q) Slides**

layer	surface roughness (nm $\pm$ $\sigma$ )	sheet resistance ( $\Omega/\square$ )
Q	$1.16 \pm 0.18$	insulator
Q/Cr/C	$0.98 \pm 0.12$	$1.4 \times 10^4$
Q/Cr/Pt	$1.08 \pm 0.21$	$8.4 \times 10^1$
Q/Cr/Pt/C	$0.88 \pm 0.10$	$6.0 \times 10^1$

**Table 2. AFM Measured Molecular Layer Thickness on Q/Cr/Pt/C and PPF Substrates<sup>a</sup>**

molecule	Q/Cr/Pt/C	PPF
NAB	$3.9 \pm 0.7$	$4.5 \pm 0.7$
AQ	$3.6 \pm 0.8$	$3.9 \pm 0.5$
FL	$1.5 \pm 0.7$	$1.7 \pm 0.4$
C <sub>10</sub>	$1.4 \pm 0.6$	$2.1 \pm 0.5$

<sup>a</sup> Thickness (nm)  $\pm$   $\sigma$ .

functions were added to the basis set to describe the Rydberg state correctly, which has been shown necessary for excited-state TDDFT calculations.<sup>32</sup> FilmStar, a dielectric thin film software, was used to calculate the effect of changing the index of refraction of the molecular layer on  $\Delta A$  spectra.<sup>33</sup>

All the junctions tested were fabricated on transparent substrates with Pt as the top contact. Junctions are labeled as "molecule/oxide", with both the substrate and the top contact omitted. For example, "NAB/SiO<sub>2</sub>" refers to a quartz/Cr/Pt/C/NAB/SiO<sub>2</sub>/Pt junction as shown in Figure 1.

## Results

The sheet resistance and surface roughness of the quartz/Cr/Pt/C substrate before and after the deposition of various substrate layers are listed in Table 1. The sheet resistance of the quartz/Cr/C substrates was three orders of magnitude higher than that of the quartz/Cr/Pt substrates. By employing Pt as a conductive sublayer, the substrates had both an acceptable resistance and a transparency while retaining carbon as the junction substrate, similar to our previously reported devices. For a typical completed junction, the resistance attributable to the substrate and top contact was  $\sim 250 \Omega$ . As noted in Table 1, the roughness of the quartz slide following deposition of Cr/Pt and Cr/Pt/C did not significantly change compared to the quartz slide itself, implying that the deposited layers were uniform. We reported previously that electron beam deposited carbon was electrochemically similar to glassy carbon and PPF allowing modification of the quartz/Cr/Pt/C substrates with diazonium reduction to proceed as expected.<sup>22</sup> Table 2 lists the thicknesses of the molecular layers formed on both quartz/Cr/Pt/C and PPF substrates showing that the resulting layer thicknesses were similar. Successful modification and high device yield reinforces the conclusion that the transparent junctions are structurally similar to the PPF junctions reported in detail.

Cyclic voltammograms of free and chemisorbed NAB and AQ in electrolytic solution are shown in Figure 2. For free NAB, two quasireversible waves centered at  $-1131$  mV ( $\Delta E_p = 81$  mV) and  $-1463$  mV ( $\Delta E_p = 112$  mV) were observed at  $0.1 \text{ V} \cdot \text{s}^{-1}$ . For chemisorbed NAB, a quasireversible wave

(30) Ingle JR., J. D.; Crouch, S. R. *Spectrochemical Analysis*; Prentice Hall: Englewood Cliffs, 1988.

(31) Frisch, M. J. T. G. W.; Schlegel, H. B.; Scuseria, G. E.; Robb, M. A.; Cheeseman, J. R.; Montgomery, J. A., Jr.; Vreven, T.; Kudin, K. N.; Burant, J. C.; Millam, J. M.; Iyengar, S. S.; Tomasi, J.; Barone, V.; Mennucci, B.; Cossi, M.; Scalmani, G.; Rega, N.; Petersson, G. A.; Nakatsuji, H.; Hada, M.; Ehara, M.; Toyota, K.; Fukuda, R.; Hasegawa, J.; Ishida, M.; Nakajima, T.; Honda, Y.; Kitao, O.; Nakai, H.; Klene, M.; Li, X.; Knox, J. E.; Hratchian, H. P.; Cross, J. B.; Bakken, V.; Adamo, C.; Jaramillo, J.; Gomperts, R.; Stratmann, R. E.; Yazyev, O.; Austin, A. J.; Cammi, R.; Pomelli, C.; Ochterski, J. W.; Ayala, P. Y.; Morokuma, K.; Voth, G. A.; Salvador, P.; Dannenberg, J. J.; Zakrzewski, V. G.; Dapprich, S.; Daniels, A. D.; Strain, M. C.; Farkas, O.; Malick, D. K.; Rabuck, A. D.; Raghavachari, K.; Foresman, J. B.; Ortiz, J. V.; Cui, Q.; Baboul, A. G.; Clifford, S.; Cioslowski, J.; Stefanov, B. B.; Liu, G.; Liashenko, A.; Piskorz, P.; Komaromi, I.; Martin, R. L.; Fox, D. J.; Keith, T.; Al-Laham, M. A.; Peng, C. Y.; Nanayakkara, A.; Challacombe, M.; Gill, P. M. W.; Johnson, B.; Chen, W.; Wong, M. W.; Gonzalez, C.; Pople, J. A. *Gaussian 03; Gaussian, Inc.*: Wallingford, CT, 2004.

(32) Kwasniewski, S. P.; Deleuze, M. S.; Francois, J. P. *Int. J. Quantum Chem.* **2000**, *80*, 672–680.

(33) FTG Software Associates: Princeton, NJ. www.ftgsoftware.com.

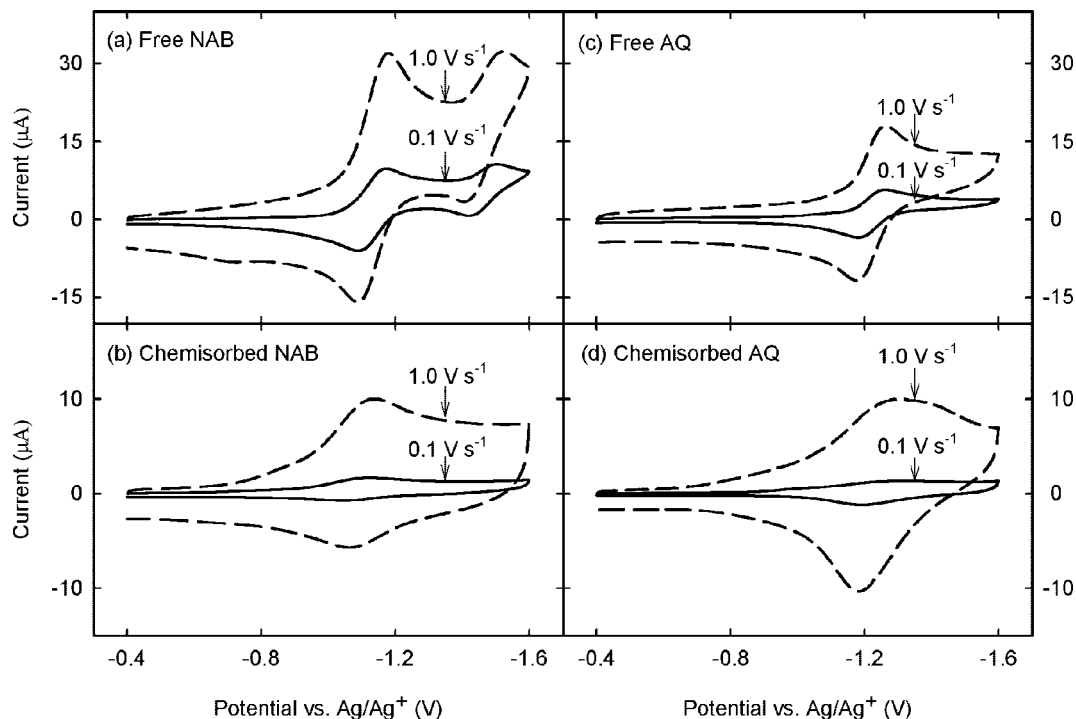


**Figure 2.** Cyclic voltammetry of free and chemisorbed molecules in MeCN containing 1.0 M TBABF<sub>4</sub> versus Ag/Ag<sup>+</sup> reference electrode: (a) 1 mM free NAB; (b) chemisorbed NAB; (c) 1 mM free AQ; and (d) chemisorbed AQ at 0.1 V·s<sup>-1</sup> (solid) and 1.0 V·s<sup>-1</sup> (dashed).

was centered at  $-1082$  mV ( $\Delta E_p = 78$  mV) for 0.1 V·s<sup>-1</sup>. For free AQ, a quasireversible wave centered at  $-1220$  mV ( $\Delta E_p = 78$  mV) was observed for 0.1 V·s<sup>-1</sup>. Chemisorbed AQ showed a quasireversible wave at  $1249$  mV ( $\Delta E_p = 115$  mV) for 0.1 V·s<sup>-1</sup>. Comparing chemisorbed NAB and AQ, the reduction peak for AQ was broadened compared to NAB. These results agree well with previous reports showing that reduction occurs within chemisorbed molecular layers in electrolyte solution.<sup>13</sup>

Optical absorbance of a transparent substrate, NAB/SiO<sub>2</sub>, and C<sub>10</sub>N/SiO<sub>2</sub> junctions are shown in Figure 3a. The maximum absorbance of all final junctions was below 1 absorbance unit (10% transmission) over the 320–820 nm range. A molecular absorbance signature was not observed in Figure 3a because the absorbance of the molecular layer is expected to be 2–3 orders of magnitude smaller than the total absorbance of the junction. Inferring the absorbance of the molecular layer by subtraction of the absorbance with and without a molecular layer leads to artifacts associated with bulk reflection and should be avoided. Absorbance of molecule/Al<sub>2</sub>O<sub>3</sub> junctions had similar absorbance magnitudes and characteristics to molecule/SiO<sub>2</sub> junctions.  $\Delta A$  versus wavelength for a  $-4$  V voltage pulse on NAB/SiO<sub>2</sub> and C<sub>10</sub>N/SiO<sub>2</sub> junctions is shown in Figure 3b. For NAB/SiO<sub>2</sub> junctions, a positive  $\Delta A$  was observed near 410 nm, a negative  $\Delta A$  near 360 nm, and a broad negative  $\Delta A$  in the 500–800 nm range.  $\Delta A$  for C<sub>10</sub>N/SiO<sub>2</sub> junctions, if any, were not observed within the LOD of the spectrometer.  $\Delta A$  of a NAB/SiO<sub>2</sub> junction increased as the magnitude of the negative voltage pulse was increased, as shown in Figure 3c. The voltage increase caused the observed  $\Delta A$  to increase with a  $\Delta A$  threshold voltage of about  $-2.5$  V. Figure 3d shows  $\Delta A$  after a  $-4$  V pulse on the NAB/Al<sub>2</sub>O<sub>3</sub> and C<sub>10</sub>N/Al<sub>2</sub>O<sub>3</sub> junctions. NAB/Al<sub>2</sub>O<sub>3</sub> junctions showed absorbance

changes similar to NAB/SiO<sub>2</sub> except for additional negative  $\Delta A$  below 330 nm and in the 600–800 nm range. These additional  $\Delta A$  trends were observed in C<sub>10</sub>N/Al<sub>2</sub>O<sub>3</sub> junctions, although on a smaller scale, providing evidence that they are caused by the Al<sub>2</sub>O<sub>3</sub> layer.

Figure 4a shows  $\Delta A$  for NAB/SiO<sub>2</sub> junctions after an initial  $-4$  V pulse and subsequent  $+4$  V pulse. The  $\Delta A$  observed in NAB/SiO<sub>2</sub> junctions after a  $-4$  V pulse was reversible with a  $+4$  V pulse causing a negative  $\Delta A$  at 410 nm, a positive  $\Delta A$  at 360 nm, and a broad positive  $\Delta A$  in the 500–800 nm range. These absorbance changes can be reversibly modulated by the polarity of the voltage pulses for at least tens of cycles, although the actual cycle lifetime was not measured. Reversible absorbance changes were also observed for NAB/Al<sub>2</sub>O<sub>3</sub> junctions. The  $\Delta A$  after a voltage pulse was stable for at least tens of minutes, as shown after a  $-4$  V pulse at 410 nm plotted versus time in Figure 4b.

Figure 5a shows  $\Delta A$  of AQ/SiO<sub>2</sub> and FL/SiO<sub>2</sub> junctions caused by a  $-4$  V pulse. AQ/SiO<sub>2</sub> junctions showed a positive  $\Delta A$  at 395 nm, negative  $\Delta A$  at 320–350 nm, and broad negative  $\Delta A$  in the 500–700 nm range. Compared to NAB/SiO<sub>2</sub> junctions, the  $\Delta A$  threshold voltage observed was 0.75 V more negative at  $-3.25$  V. Similar to the C<sub>10</sub>N/SiO<sub>2</sub> junctions, FL/SiO<sub>2</sub> junctions did not have an observable absorbance change for applied voltage pulses up to  $\pm 4.0$  V. Figure 5b shows  $\Delta A$  decay for AQ/SiO<sub>2</sub> junctions after a  $-4$  V pulse, indicating a complete decay in  $\sim 10$  s. Since the RC time constant of the junctions and voltage pulse length were shorter than the spectrometer's integration time, the observed  $\Delta A$  was not caused by electroreflectance changes during the voltage pulse.

TDDFT calculated energies, several selected calculated absorption wavelengths, and experimentally reported absorption wavelengths for NAB, NAB radical anion, AQ, and AQ

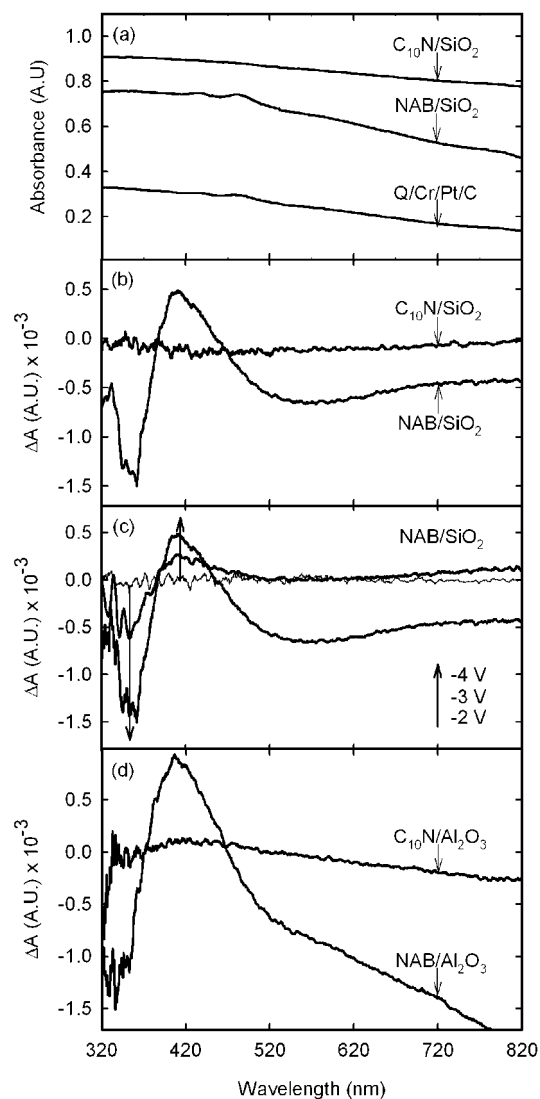


**Figure 3.** (a) Absorbance of a transparent substrate, NAB/SiO<sub>2</sub>, and AQ/SiO<sub>2</sub> junctions; (b)  $\Delta A$  of NAB/SiO<sub>2</sub> and C<sub>10</sub>N/SiO<sub>2</sub> after a -4 V, 100 ms pulse; (c)  $\Delta A$  of NAB/SiO<sub>2</sub> for negative voltage pulses of -2 V, -3 V, and -4 V; (d)  $\Delta A$  of NAB/Al<sub>2</sub>O<sub>3</sub> and C<sub>10</sub>N/Al<sub>2</sub>O<sub>3</sub> after a -4 V, 100 ms pulse.

radical anion are listed in Table 3. Although the calculated oscillator strengths could be used as an indication of the absorbance strength, correlation between these calculated values and experimental measurements is generally poor, especially for radical anions.<sup>34</sup> Considering the molecules are self-solvated, attached to a surface, and exposed to electric fields of several MV·cm<sup>-1</sup>, the reported excitation energy should be used as a general reference. An important conclusion is the calculated absorbance wavelength of the radical anion was red-shifted compared to the neutral species for both NAB and AQ. This conclusion is supported with previously reported absorption values of NAB and AQ anions in electrolytic solution.<sup>35–37</sup> The calculated energies show both anions are more stable compared to their neutral state in the gas phase: NAB anion is 1.90 eV more stable than NAB and AQ anion is 1.36 eV more stable than AQ.

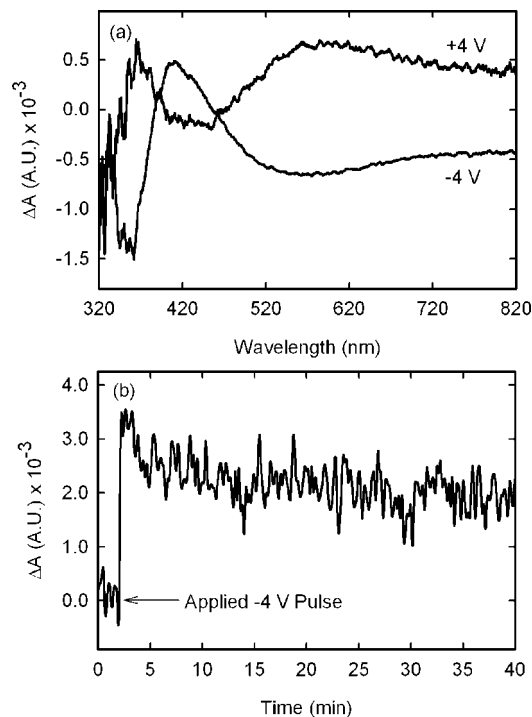


**Figure 4.** (a)  $\Delta A$  of NAB/SiO<sub>2</sub> after a -4 V pulse and subsequent +4 V pulse.  $\Delta A$  of the two voltage pulses are nearly symmetric about zero  $\Delta A$ ; (b)  $\Delta A$  of a NAB/SiO<sub>2</sub> at 410 nm before and after a -4 V pulse. The increase in  $\Delta A$  at  $t = 2$  min was caused by the application of the -4 V pulse.

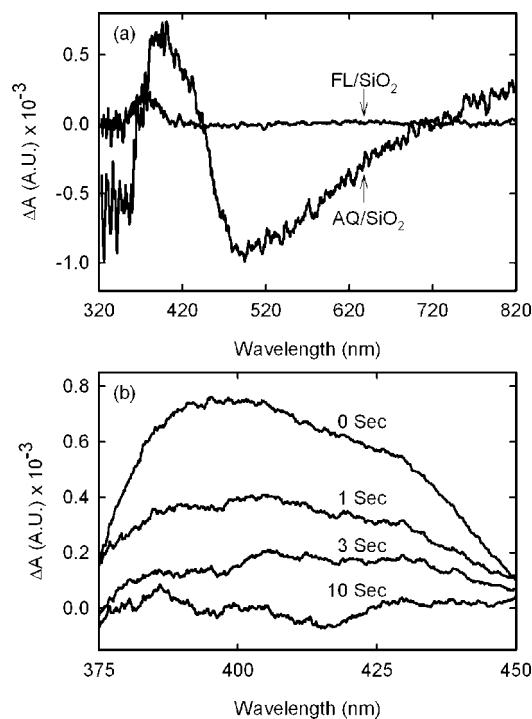


**Figure 5.** (a)  $\Delta A$  of AQ/SiO<sub>2</sub> and FL/SiO<sub>2</sub> after a -4 V, 100 ms pulse; (b)  $\Delta A$  of AQ/SiO<sub>2</sub> after a -4 V pulse as a function of time.

## Discussion

For C<sub>10</sub>N/SiO<sub>2</sub> junctions,  $\Delta A$  in response to a voltage pulse was below the LOD in the range of  $\pm 4$  V.  $\Delta A$  caused by redox activity of the C<sub>10</sub>N layer was not expected in both the measured wavelength and the applied voltage range. Since SiO<sub>2</sub> has an optical band gap larger than the measured

(34) DiLabio, G. A.; Litwinienko, G.; Lin, S. Q.; Pratt, D. A.; Ingold, K. U. *J. Phys. Chem. A* **2002**, *106*, 11719–11725.

**Table 3. Calculated Total Energies (Gas Phase), Selected Calculated Excitation Wavelengths (Gas Phase), and Experimentally Measured Excitation Wavelengths (Solution) of NAB, NAB Anion, AQ, and AQ Anion<sup>a</sup>**

molecule	energy (E-h)	calculated wavelengths, free molecule [oscillator strength] (nm)	experimental wavelengths [solvent] (nm)
NAB	-777.31	340.2 [0.05]; 343.6 [0.00]; 368.6 [0.83]; 511.3 [0.00]	330 [MeCN] <sup>32</sup>
NAB anion	-777.38	352.0 [0.08]; 408.8 [0.60]; 850.0 [0.32]	490 [MeCN] <sup>32</sup>
AQ	-688.82	324.9 [0.12]; 340.5 [0.00]; 384.8 [0.00]; 420.13 [0.00]	270, 320 [DMF] <sup>30,31</sup>
AQ anion	-688.87	363.1 [0.02]; 407.7 [0.00]; 568.0 [0.18]	274, 390, 410, 556 [DMF] <sup>30,31</sup>

<sup>a</sup> A complete list of the calculated excitation wavelengths is located in Supporting Information.

spectral range, an observable  $\Delta A$  was also not expected for the SiO<sub>2</sub> layer. Although the deposited SiO<sub>2</sub> layer was not crystalline, high O<sub>2</sub> backpressure during deposition has been shown to create near stoichiometric films.<sup>38,39</sup> The absence of a detectable  $\Delta A$  in the C<sub>10</sub>N/SiO<sub>2</sub> case allows three critical conclusions to be drawn. First, C<sub>10</sub>N and SiO<sub>2</sub> can be used as "controls" which do not exhibit voltage dependent optical responses in the wavelength range investigated. Second, changes in transmission due to voltage induced electroreflectance changes in the electrodes were not observed and, therefore, are smaller than the LOD. Third, the intensity of the single beam spectrometer is at least stable for the several minutes required for spectrum acquisition.

Similar to C<sub>10</sub>N/SiO<sub>2</sub> junctions,  $\Delta A$  for FL/SiO<sub>2</sub> was below the LOD. The lack of an observed absorbance change indicates that either the FL layer is not redox active in the applied voltage range or the absorbance changes associated with the reduction of the FL layer are too small to measure. The reported reduction potential for FL is -3.05 V versus a Ag/Ag<sup>+</sup> electrode indicating that reduction of the FL layer would be significantly less likely compared to NAB and AQ layers.<sup>40</sup> In addition, FL has a calculated lowest unoccupied molecular orbital (LUMO) at -1.07 eV which is about 3.8–4.0 eV above the Fermi level of the carbon substrate. Considering this large mismatch between the Fermi level of the carbon substrate and the LUMO of FL, limited electron transfer between the two layers would be expected in the  $\pm 4$  V range.

Based on the voltammetric results, NAB and AQ were shown to be electrochemically reducible as free molecules and chemisorbed on a carbon surface. When the molecular layer in a solid state junction consisted of either of these molecules, voltage dependent absorbance changes were observed. If reduction of the NAB layer occurred, the positive  $\Delta A$  at 410 nm would be consistent with the formation of NAB anions and the negative  $\Delta A$  at 360 nm with the loss of neutral NAB. This observed red shift in absorption is consistent with the TDDFT calculations, which predicts a red shift upon formation of the NAB anion compared to the neutral NAB molecule. Comparable absorption changes were

observed in NAB/Al<sub>2</sub>O<sub>3</sub> junctions indicating the absorption changes at 360 and 410 nm were not caused by the SiO<sub>2</sub> or Al<sub>2</sub>O<sub>3</sub> layers. If the AQ layer underwent reduction, the positive  $\Delta A$  at 395 nm would be consistent with the formation of AQ anions and the negative  $\Delta A$  at 320–350 nm with the loss of neutral AQ. Although the AQ anion did not have a calculated absorption at 395 nm, reduction of the AQ layer is probable. The calculated AQ LUMO (-3.17 eV) has only a slightly higher energy than the NAB LUMO (-3.43 eV). Compared to NAB/SiO<sub>2</sub> junctions, AQ/SiO<sub>2</sub> had a more negative  $\Delta A$  threshold voltage. These results are consistent with the cyclic voltammetric results where chemisorbed AQ reduction occurred at a slightly more negative potential compared to chemisorbed NAB reduction.

For NAB/SiO<sub>2</sub> junctions, the application of a positive voltage pulse after a negative voltage pulse caused a positive  $\Delta A$  at 360 nm and a negative  $\Delta A$  at 410 nm. These absorbance changes are opposite to the absorbance changes after a negative voltage pulse and are consistent with the reoxidation of the NAB layer during the positive voltage pulse. Since a positive  $\Delta A$  at 360 nm and a negative  $\Delta A$  at 410 nm after a positive voltage pulse were observed, the initial NAB layer appears to have been partially reduced. Previous Raman spectrometry on similar devices has provided evidence that the initial NAB layer is partially reduced during either diazonium reduction or deposition of the oxide layer.<sup>41</sup> Since  $\Delta A$  can be cycled for at least tens of cycles, the reduction and subsequent oxidation of the NAB layer is consistent with a chemically reversible redox process in a solid state device.

For both NAB/SiO<sub>2</sub> and AQ/SiO<sub>2</sub> junctions, a negative  $\Delta A$  was observed in the 500–800 nm range after the application of a negative voltage pulse. Since NAB, AQ, and their anions are not expected to have optical absorption in this wavelength region,  $\Delta A$  could be the result of intermolecular interactions or the change in the index of refraction of the molecular layer. Reduction of NAB and AQ was calculated to significantly increase their polarizability and thus increase the index of refraction of their respective molecular layer. Calculations with FilmStar showed a change in the index of refraction of the molecular layer in carbon/molecule/SiO<sub>2</sub>/Pt junctions could result in a broad negative  $\Delta A$  in the red region of the spectrum. Considering both absorption and index of refraction changes of the molecular layer upon reduction,  $\Delta A$  of the molecular layers has two classifications: molecular absorption changes and molecular index of refraction changes. Both of these

(35) Pedersen, S. U.; Christensen, T. B.; Thomasen, T.; Daasbjerg, K. *J. Electroanal. Chem.* **1998**, *454*, 123–143.

(36) Shamsipur, M.; Hemmateenejad, B.; Babaei, A.; Faraj-Sharabiani, L. *J. Electroanal. Chem.* **2004**, *570*, 227–234.

(37) Tian, H.; Bergren, A. J.; McCreery, R. L. *Appl. Spectrosc.* **2007**, in press.

(38) Khodier, S. A.; Sidki, H. M. *J. Mater. Sci.: Mater. Electron.* **2001**, *12*, 107–109.

(39) Rao, K. N.; Shivlingappa, L.; Mohan, S. *Mater. Sci. Eng., B* **2003**, *98*, 38–44.

(40) Jezorek, J. R.; Lagu, A.; Seigel, T. M.; Mark, H. B. *J. Org. Chem.* **1973**, *38*, 788–795.

(41) Nowak, A. M.; McCreery, R. L. *Anal. Chem.* **2004**, *76*, 1089–1097.

changes should be considered during the analysis of in-situ optical absorbance spectra.

Although both NAB/SiO<sub>2</sub> and AQ/SiO<sub>2</sub> junctions showed evidence for solid state reduction, the persistence of the observed  $\Delta A$  differed by at least 2 orders of magnitude.  $\Delta A$  after a voltage pulse was observed for at least tens of minutes with NAB/SiO<sub>2</sub> junctions but for only several seconds with AQ/SiO<sub>2</sub> junctions. In the cyclic voltammetric results, the reduction peak of chemisorbed AQ was broader compared to that of chemisorbed NAB which has been reported to be an indication that chemisorbed AQ anions are less stable compared to chemisorbed NAB anions.<sup>42–44</sup> The NAB anion had higher stability than the AQ anion when compared to their respective neutral states in TDDFT calculations. These two results are consistent with a more stable NAB anion layer, but there may be other factors which affected the  $\Delta A$  persistence. One additional explanation is the reduced molecular layers are stabilized by the presence of point defects or counterions. Since the oxide layer was deposited by electron beam evaporation, point defects are expected to be present in the oxide films. In addition, the application of high electric fields can cause the formation of additional point defects and the rearrangement of counterions. Complexing of the reduced molecular state with either point defects or counterions would add additional stability to the reduced molecular layer. For the NAB anion, the highly negative NO<sub>2</sub> group could complex with point defects efficiently at the molecular/oxide interface. For the AQ anion, the carbonyl groups located in the center of the molecule are less likely to interact with point defects in the oxide based on the lack of spatial interaction with the oxide layer. Via one or more of the above explanations, the persistence of  $\Delta A$  was strongly dependent on the molecule composing the molecular layer.

(42) Bard, A. J.; Faulkner, L. R. *Electrochemical Methods Fundamentals and Applications*, 2nd ed.; John Wiley: New York, 2001.

(43) Matsuda, H.; Aoki, K.; Tokuda, K. *J. Electroanal. Chem.* **1987**, *217*, 1–13.

(44) Matsuda, H.; Aoki, K.; Tokuda, K. *J. Electroanal. Chem.* **1987**, *217*, 15–32.

## Conclusions

Overall, these results provide experimental evidence that molecular energy levels within a carbon/molecule/oxide/Pt junction can be dynamically changed by an applied bias. Understanding how these energy levels change will provide a more complete understanding of the electronic behavior of molecular devices. As indicated in the discussion, additional experiments are needed and are currently in progress to more completely identify the following: stability of reduced molecular layers, charge injection mechanisms, and the effect of an applied bias on redox active oxide layers such as TiO<sub>2</sub>. In-situ optical absorption spectroscopy was shown to be applicable for NAB and AQ molecular junctions; for example, AQ could not be analyzed with Raman spectroscopy because of its weak Raman scattering. As an additional diagnostic tool, optical absorption spectroscopy can be used in-situ to probe the molecular layer “buried” within a molecular junction. We anticipate that UV–vis–NIR absorption spectroscopy in both static and transient modes will provide important insights into structural changes and electronic behavior of working molecular junctions under an applied bias.

**Acknowledgment.** The authors would like to thank Haijun Yan for his help with the modification of carbon substrates. This work was supported by the National Science Foundation through Project No. 0211693 from the Analytical and Surface Chemistry Division, The National Research Council of Canada, Natural Science and Research Council of Canada, and the Alberta Ingenuity Fund.

**Supporting Information Available:** Current–voltage curves for C<sub>10</sub>N/SiO<sub>2</sub> and NAB/SiO<sub>2</sub> junctions showing the capacitance nature of the junctions and the effect of the voltage pulses; a complete table of the calculated TDDFT excitation energies and oscillator strengths (PDF). This material is available free of charge via the Internet at <http://pubs.acs.org>.

CM703614N